

UNCLASSIFIED

492603

# BALLISTIC RESEARCH LABORATORIES

5- JUL 1996

REFERENCE COPY  
DOES NOT CIRCULATE



**Report No. 601**

## **Supersonic Wind Tunnel Tests on Four Wings With Sweepback**

PROPERTY OF U.S. ARMY  
STINFO BRANCH  
BRL, APG, MD. 21005

**ALLEN E. PUCKETT**

Approved for Public  
Release; distribution is  
unlimited

**ABERDEEN PROVING GROUND, MARYLAND**

# **BALLISTIC RESEARCH LABORATORIES**

**REPORT NO. 601**

**Project No. 5117**

**SUPERSONIC PROBLEM NO. SS-2**

## **Supersonic Wind Tunnel Tests on Four Wings with Sweepback**

PROPERTY OF U.S. ARMY  
STINFO BUREAU  
ABERDEEN PROVING GROUND  
MD. 21005

**ALLEN E. PUCKETT**

**24 September 1945**

**ABERDEEN PROVING GROUND, MARYLAND**

TABLE OF CONTENTS

	Page
ABSTRACT -----	3
GENERAL -----	4
DISCUSSION OF LIFT CHARACTERISTICS -----	8
DISCUSSION OF DRAG CHARACTERISTICS -----	11
Drag at Zero Lift -----	11
Drag Due to Lift -----	12
LIFT DRAG RATIOS -----	13
SCHLIEREN OBSERVATIONS OF FLOW -----	16
GRAPHS- 14-18 -----	19
TABLE OF NOMENCLATURE -----	24

**BALLISTIC RESEARCH LABORATORIES****REPORT NO. 601**

Project No. 5117

Puckett/mar  
Aberdeen Proving Ground, Md.**Supersonic Problem  
No. SS-2****SUPERSONIC WIND TUNNEL TESTS ON FOUR WINGS WITH SWEEPBACK****ABSTRACT**

Tests of four airfoils with sweepback angles of  $0^\circ$ ,  $30^\circ$ ,  $60^\circ$ ,  $67.5^\circ$  at a Mach number of 1.72 are compared with a simple theory. It is shown that little improvement in the lift-drag ratio is produced until the airfoil lies inside the Mach angle, but that the L/D ratio may be almost doubled using the proper sweepback angle.

## SUPersonic WIND TUNNEL TESTS ON FOUR WINGS WITH SWEEPBACK

### GENERAL

It was pointed out by Busemann<sup>1</sup> that the forces on a two-dimensional wing of infinite span placed at an angle to the flow can be computed by regarding the free stream velocity to consist of two components, one normal to the leading edge of the airfoil, and one parallel to it. (See Fig. 1.) The forces are then determined entirely by the normal component; the parallel component has no effect. The angle of sweepback,  $\sigma$ , may be such that the normal velocity component is less than the speed of sound, i.e.,  $\sigma > \mu$ , where  $\mu$  is the complement of the Mach angle  $\theta$ , and

$$\theta = \sin^{-1} (1/Ma)$$

The forces on the wing should then be characteristic of subsonic speeds, and an improvement in performance, specifically in the ratio of lift to drag, may be expected. For an airfoil of finite span, due to conditions at the center section and at the tips, departures from the simple two-dimensional predictions are expected.

<sup>1</sup> Volta Congress, Proceedings, 1935; "Aerodynamischen Auftrieb bei Überschallgeschwindigkeit."

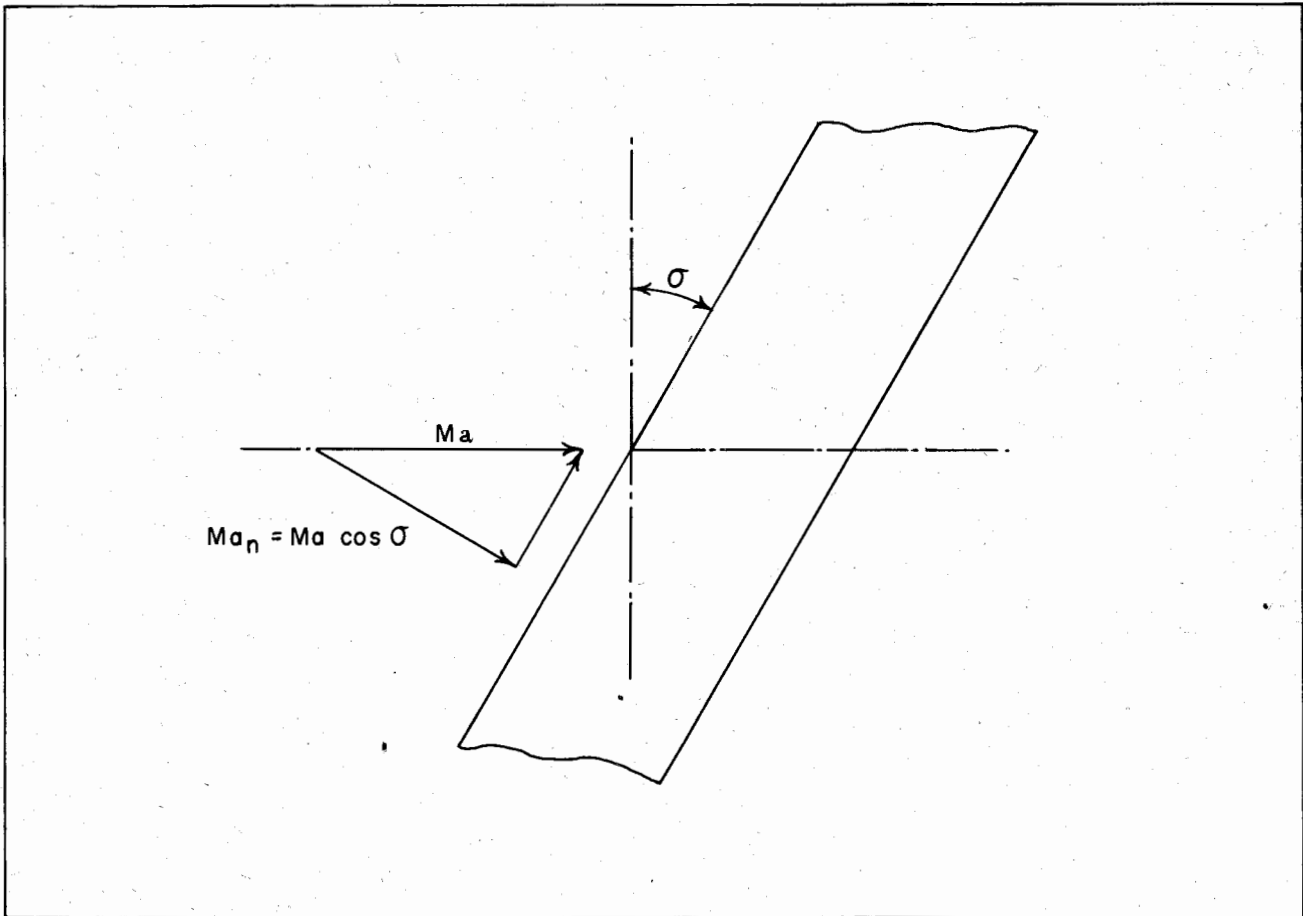


FIG. 1

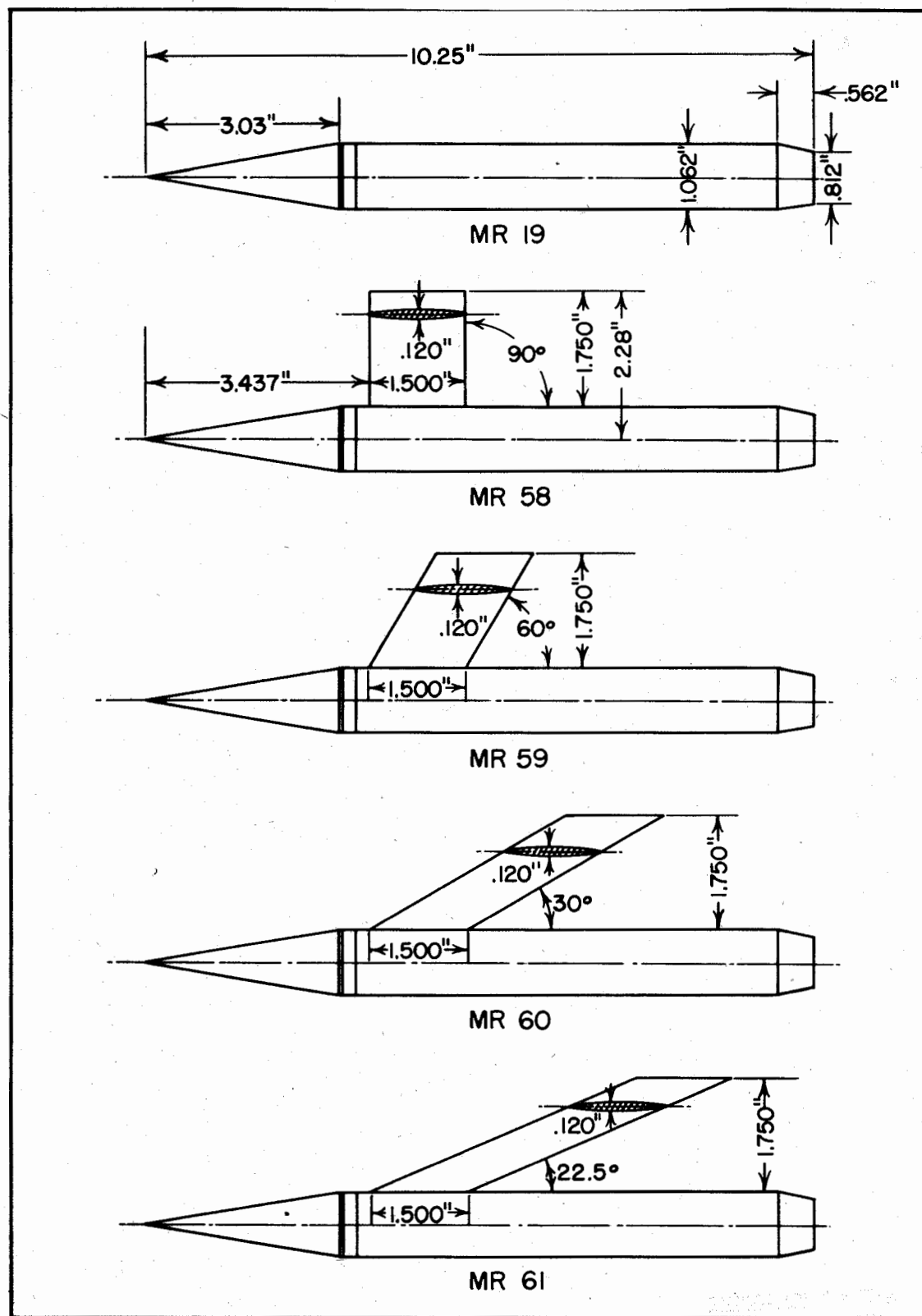


FIG. 2

In order to check this, at least qualitatively, four airfoils were constructed with varying sweep-back angles. These were tested in the Aberdeen Bomb Tunnel at a Mach number of  $M = 1.72$ . The four sweepback angles used were  $\sigma = 0^\circ, 30^\circ, 60^\circ$ , and  $67.5^\circ$ . If the "normal Mach number",  $Ma_n$ , is defined as

$$Ma_n = Ma \cos \sigma$$

the values of  $Ma_n$  for these wings are given in Table I.

Table I

$\sigma$	$0^\circ$	$30^\circ$	$60^\circ$	$67.5^\circ$
$Ma_n$	1.72	1.49	.86	.66

It will be noted that  $Ma_n$  for the last two airfoils is subsonic; the Mach angle for  $Ma = 1.72$  is  $35.5^\circ$ .

To simplify testing, the models were attached to a cylindrical body with a conical nose ( $20^\circ$  Apex angle). Thus the results reported herein apply to such a wing-body combination, and include all interference effects such as change in pressure distribution over the body due to the wing. The airfoil section was maintained constant at the root, — a bi-convex symmetrical circular arc section with thickness ratio of 8%. The wing span was also kept constant, and thus also the wing area. The four plan-forms tested are shown in Fig. 2.

The method of testing was identical to that used in the tests of the Calibration models, which is described in an earlier Ballistic Research Laboratory Report<sup>2</sup>. The models were supported in the test section of the Bomb Tunnel by means of a single strut from the rear. This strut was shielded up to the base of the model, so there were no tare forces. The pressure acting over the base of the model was measured and recorded.

Force coefficients were first computed according to the definitions

$$C_D = \frac{D}{1/2 \rho u^2 d^2} \quad (1)$$

$$C_L = \frac{L}{1/2 \rho u^2 d^2} \quad (2)$$

$$C_{Mb} = \frac{M_b}{1/2 \rho u^2 d^3} \quad (3)$$

where  $D$ ,  $L$ ,  $M_b$  are drag, lift, and moment about the base of the model respectively, and  $d$  is the diameter of the model. An additional force coefficient was defined for the forward force acting over the base of the model,

$$C_{FB} = \frac{\rho_b d'^2 \pi}{1/2 \rho u^2 d^2 4}$$

where  $d'$  is the model diameter at its base. By adding  $C_{FB}$  to the drag coefficient in Eq. 1, the effective

<sup>2</sup> Puckett-Emmons, "Bomb Tunnel Tests Nozzle M-1.7", BRL Report No. 541, Aberdeen Proving Ground, 5 April 1945.

drag coefficient at zero pressure on the model base is determined. The drag of the wings above was then determined as the difference between drags of the model with and without wings, reduced to zero base pressure, so that any effect of the wings on this base pressure was eliminated. The force coefficients determined for the complete models are given in Figs. 14 and 15.

The lift and moment of the wings above were determined also as the difference between runs with and without wings. These forces are reported in coefficients based on the actual projected area of the wings, rather than the body diameter squared. The "center-section" area of the wing, through the body, is not included. Then

$$C_D = \frac{D}{1/2 \rho u^2 A} \quad (4)$$

$$C_L = \frac{L}{1/2 \rho u^2 A} \quad (5)$$

$$C_{Mo} = \frac{M_o}{1/2 \rho u^2 A c} \quad (6)$$

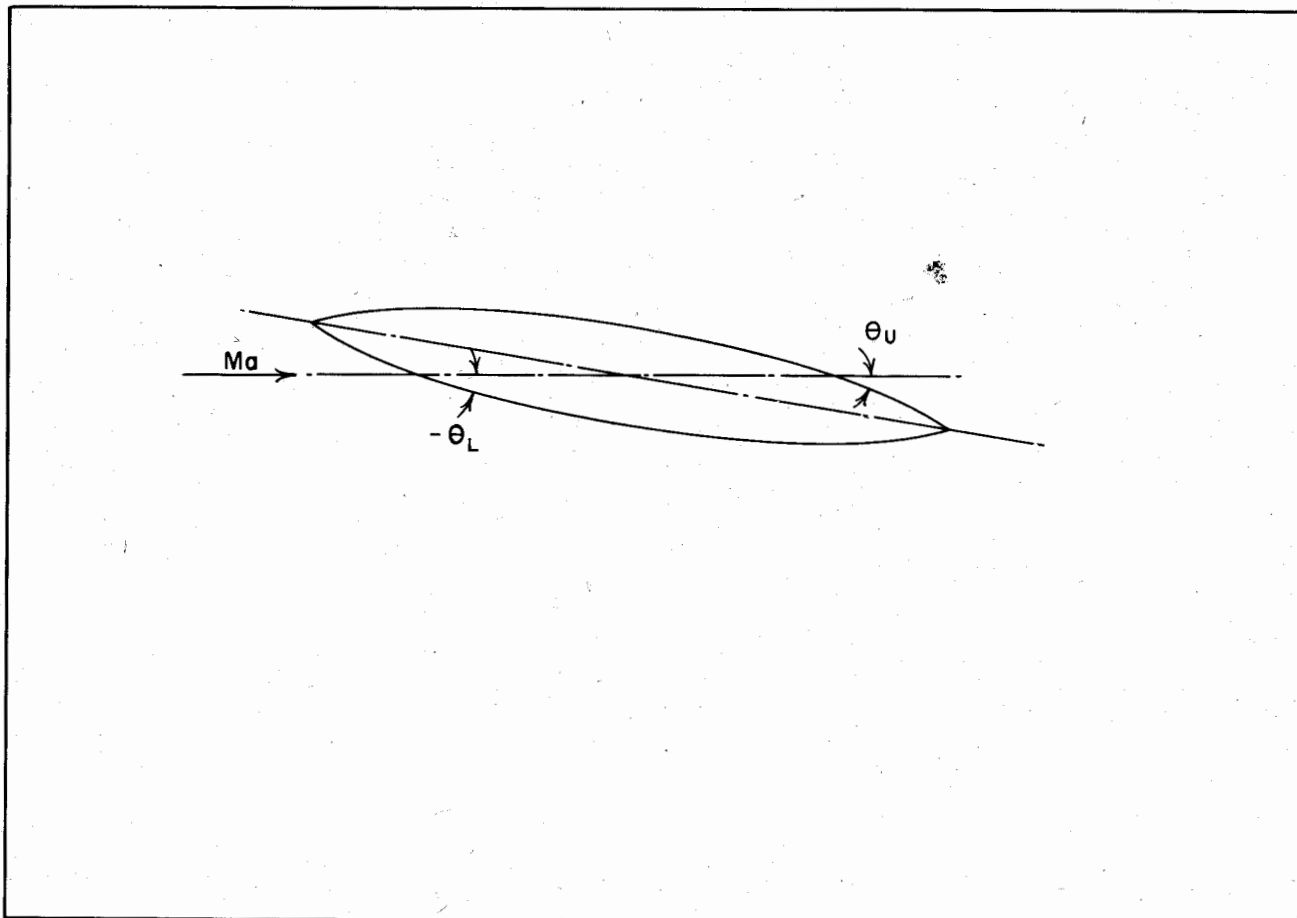


FIG. 3

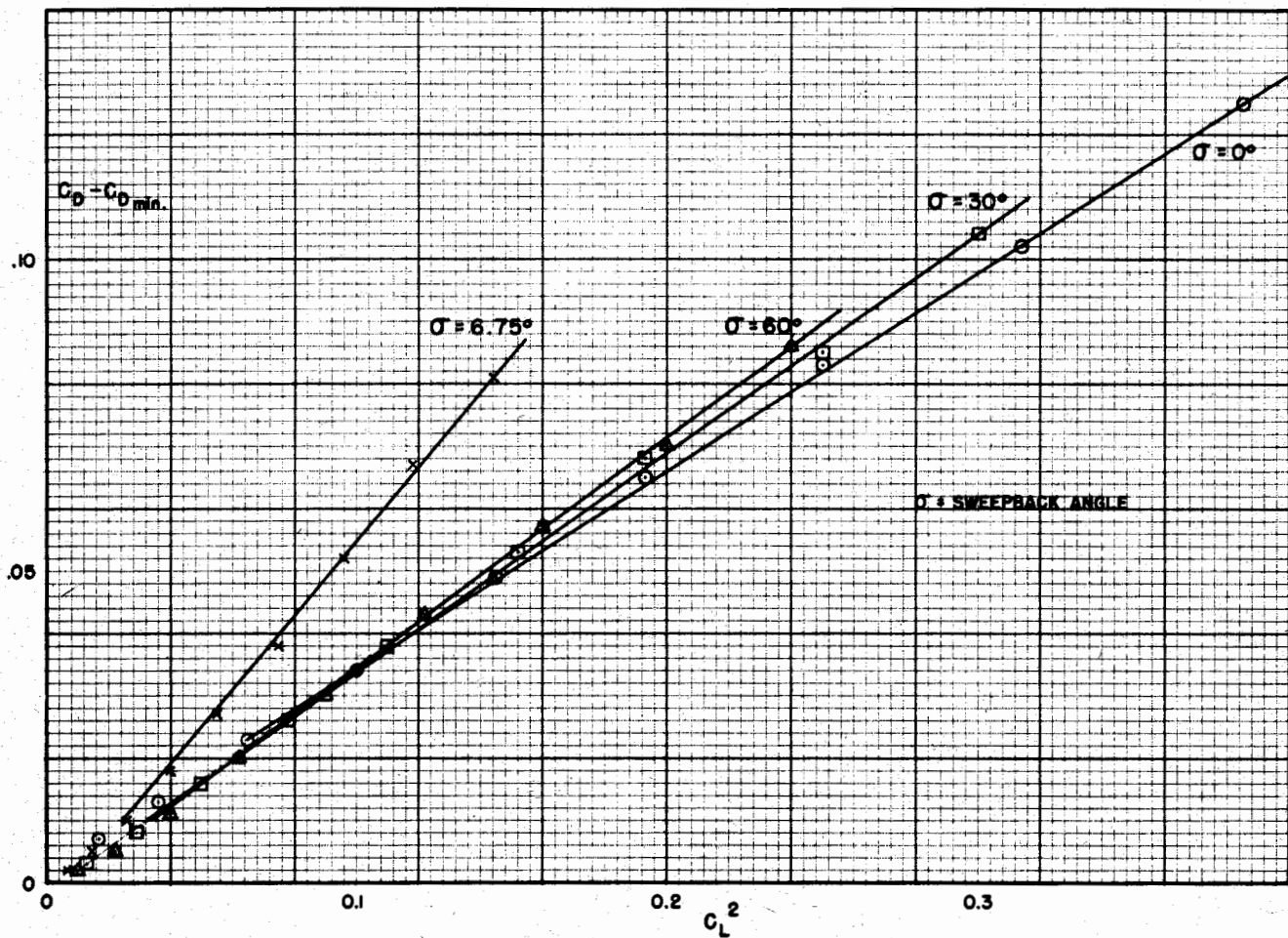


Fig. 4

where  $A$  = wing area, and  $c$  = wing chord. The forces  $L$  and  $D$  are here understood to be the increments due to the wing. The moment was computed about a lateral axis through the center of the root chord. The drag, lift, and moment coefficients so determined are plotted in Figs. 16 and 17.

The ratio of lift to drag for wing only, determined from Figs. 16 and 17, is plotted in Fig. 18. It will be noted there that the maximum  $L/D$  was obtained with a sweepback of  $\sigma = 67.5^\circ$ , and  $Ma_n = .66$ , and was approximately 80% larger than that obtained with zero sweepback.

#### DISCUSSION OF LIFT CHARACTERISTICS

In order to discuss the forces on the airfoil in terms of the flow normal to its leading edge, a "normal lift coefficient",  $C_{Ln}$  may be defined by means of

$$L = \frac{1}{2} \rho u_n^2 C_{Ln} A = \frac{1}{2} \rho u^2 (\cos^2 \sigma) C_{Ln} A$$

Using Eq. 5, we see that

$$C_{Ln} = \frac{C_L}{\cos^2 \sigma}$$

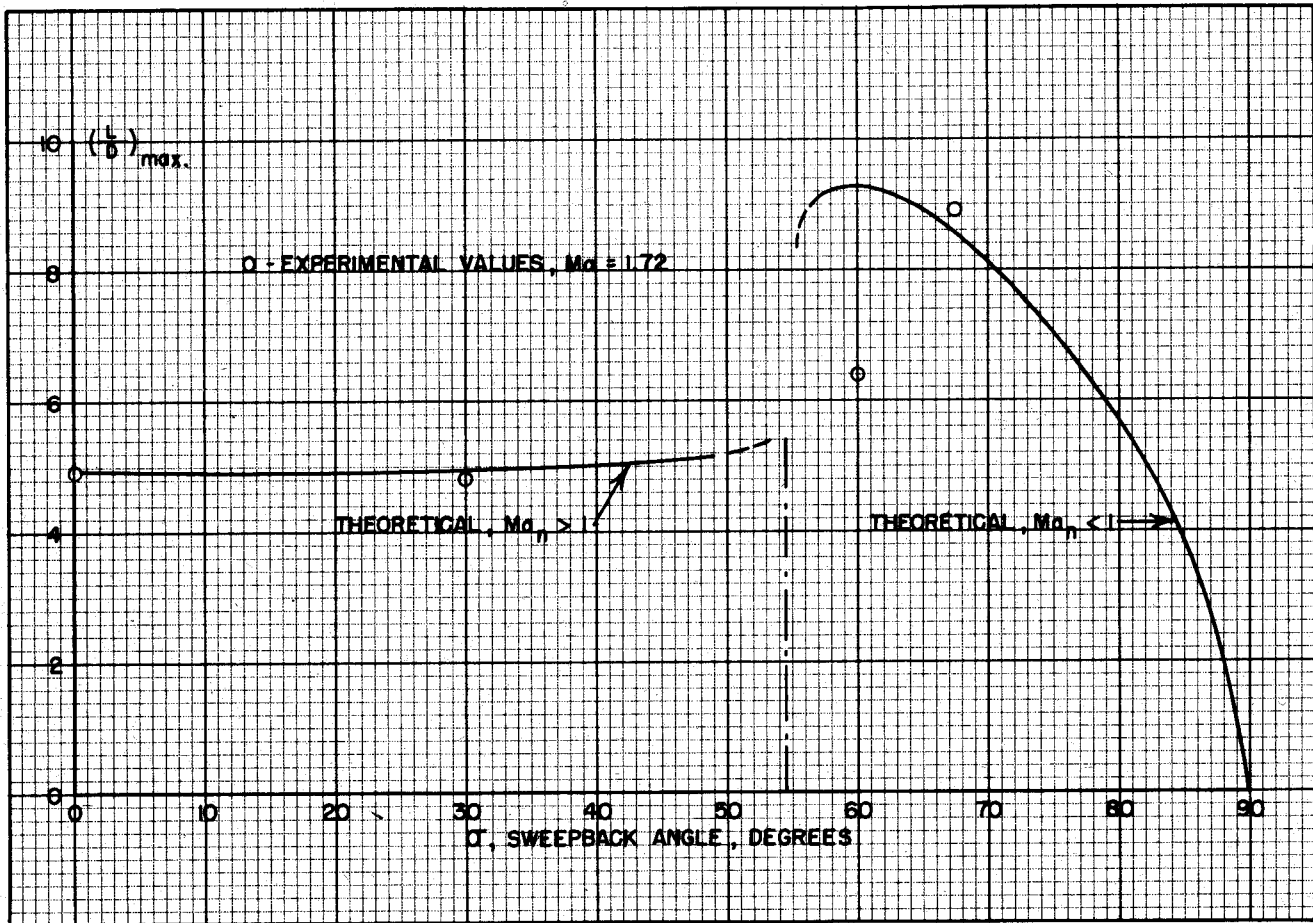


FIG. 5

Also the "normal lift coefficient" will presumably be a function of the angle of attack of the wing relative to the normal velocity component. If  $\alpha_n$  is the "normal" angle of attack, and  $\alpha$  the angle of attack relative to the true velocity, then

$$\alpha_n = \frac{\alpha}{\cos \sigma} \quad (8)$$

The slope of the lift curve referred to the normal flow is then related to the true lift curve slope by

$$\frac{d C_{Ln}}{d \alpha_n} = \frac{d C_L}{d \alpha} \cdot \frac{1}{\cos \sigma} \quad (9)$$

For a supersonic, two-dimensional airfoil, the slope of the lift curve, according to the first-order theory is given by

$$\frac{d C_L}{d \alpha} = \frac{4}{\sqrt{Ma^2 - 1}} \quad (10)$$

In the sweepback case, it is expected that  $d C_{Ln}/d \alpha_n$  might follow this law, substituting  $Ma_n$  for  $Ma$  in Eq. 10, i.e.,

$$\frac{d C_{Ln}}{d \alpha_n} = \frac{4}{\sqrt{Ma_n^2 - 1}} = a_s \quad (10a)$$

In the case of a subsonic airfoil with no sweepback, the slope of the lift curve is given approximately by

$$\frac{d C_L}{d \alpha} = \frac{2\pi}{1+2/AR} = a_u \quad (11)$$

where AR = aspect ratio, and compressibility has been neglected. In the case of a finite, swept-back air-

foil, it is difficult to say what effective aspect ratio should be used. It is clear that the presence of the wing tips is made known to the flow only within the Mach cone following each tip, which includes very little of the air foil. The effect of the center section is certainly felt over the entire wing.

For a preliminary comparison, the subsonic lift curve slope may be computed for AR = infinity. In Table II are given values of  $dC_L/d\alpha$  determined in the wind tunnel for the true velocity, and also referred to the normal flow, as given by Eq. 9. The theoretical supersonic and subsonic lift curve slope, from Eqs. 10a and 11 are given; the slopes listed, however, are per degree, instead of per radian, as in Eqs. 10a and 11.

Table II

$\sigma$	Ma <sub>n</sub>	$\frac{dC_L}{d\alpha}$	$\frac{dC_{Ln}}{d\alpha_n}$	a <sub>s</sub>	a <sub>u</sub>
(Experiment)					
0	1.72	.062	.062	.050	---
30°	1.49	.056	.065	.063	---
60°	.86	.060	.100	---	.110
67.5	.66	.039	.102	---	.110

It will be noticed that the experimental normal lift coefficients compare very well with the theoretical in all cases but  $\sigma = 0^\circ$ . There are two possibilities for the discrepancy in this case; the pressure distribution over the body may be altered to the extent that the center section is contributing some appreciable lift, or the thickness of the airfoil is such that the 1st order theory does not accurately predict results. The second possibility may be checked by making an exact computation of the flow over the upper and lower surfaces of the airfoil, using the Prandtl-Meyer relations giving Mach number and pressure as a function of flow direction only. Such a computation is valid for this type of effectively "single walled" flow — i.e., only one family of characteristics exists on each side of the airfoil. If  $\theta$  is the flow inclination relative to the free stream at any point on the airfoil surface, measured clockwise on the upper surface and counterclockwise on the lower surface (See Fig. 3), then

$$\theta + \theta_0 = \sqrt{(\gamma + 1)/(\gamma - 1)} \tan^{-1}(\sqrt{(\gamma - 1)/(\gamma + 1)} \sqrt{Ma^2 - 1}) - \tan^{-1} \sqrt{Ma^2 - 1} \quad (12)$$

where  $\theta_0$  is the value of the right-hand side of Eq. 12 at the free stream Mach number. Here Ma is the local Mach number at any point on the airfoil surface. The local pressure is a function of local Mach number, given by

$$\frac{P}{P_0} = (1 + \frac{\gamma - 1}{2} Ma^2)^{-\frac{1}{\gamma - 1}}$$

The lift is determined as the integral of this pressure around the airfoil.

Another check on the effect of thickness on the two-dimension airfoil characteristics may be made using the third order theory developed by A. Busemann<sup>3</sup>. This theory amounts essentially to an expansion of Eq. 12 up to the third power of  $\theta$ . Both this computation and the Prandtl-Meyer computation were made for an airfoil of 10% thickness at Ma = 1.72, with a bi-convex symmetrical circular arc cross section. The

<sup>3</sup> Busemann, Volta Congress 1935, loc. cit.

effect of the finite shock wave was neglected in both, but it will have the effect of lowering the lift very slightly. The results are compared with the first order theory in Table III, where  $d C_L/d\alpha$  per degree is tabulated.

Table III

	$d C_L/d\alpha$
1st order theory	.050
3rd order theory	.051
Prandtl-Meyer theory	.052

It is seen that the effect of the finite deflection of the flow is very small, and can hardly account for the large lift of the  $\sigma = 0^\circ$  wing. For this wing, the ratio of center-section area to exterior wing area is 30%. Since the measured lift is about 20% higher than the theoretical lift based on exterior wing area, it might be concluded that the center section is contributing lift, but only about 70% as effectively as the exterior airfoil.

There is no apparent reason why this center section lift should exist for the  $\sigma = 0^\circ$  wing, but not for any of the others. In the case of the  $\sigma = 60^\circ$  wing, since  $Ma_n = .86$ , it might be expected that some compressibility effects would be evident in the normal flow. However, both that wing and the  $\sigma = 67.5^\circ$  wing produced normal lift curve slopes conforming closely to conventional subsonic values.

### DISCUSSION OF DRAG CHARACTERISTICS

#### Drag at Zero Lift.

The drag coefficients as measured and referred to the true air velocity may also be referred to the flow normal to the wing in the same manner as the lift. It must be observed, however, that the drag produced by a flow purely normal to the wing is also in a direction normal to the leading edge; the component of this normal drag in the direction of the true air velocity is less by the factor  $\cos \sigma$ . In addition, the wing experiences a skin-friction drag associated with the true air velocity. The total drag then consists of

$$D = 1/2 \rho u_n^2 C_{Dn} A \cos \sigma + 2C_f 1/2 \rho u^2 A \quad (13)$$

where  $C_f$  is the skin friction coefficient. Using Eq. 4, we obtain

$$CD = C_{Dn} \cos^3 \sigma + 2C_f \quad (14)$$

For the angles  $\sigma = 0^\circ$  and  $\sigma = 30^\circ$ , with the normal Mach number larger than 1.0, the coefficient of normal drag should be the wave drag coefficient associated with the normal flow. This coefficient, as given by Busemann for a circular arc, symmetrical section, is

$$C_{Dn} = \frac{16}{3} \frac{t_n^2}{\sqrt{Ma_n^2 - 1}} \quad (15)$$

where  $t_n$  is the thickness ratio of the airfoil, measured normal to the chord. If  $t$  is the thickness ratio relative to a longitudinal section of the wing, then

$$t_n = \frac{t}{\cos \sigma} \quad (16)$$

The friction coefficient should have a value of approximately  $C_f = .003$ . The normal drag coefficient for the cases  $\sigma = 60^\circ$  and  $67.5^\circ$  should correspond to subsonic drag coefficients at  $Ma = .86$  and  $.66$  respectively. It is difficult to evaluate these last two, but at high sweepback angles it is seen from Eq. 14 that their effect becomes small anyway. In Table IV are summarized the results of a computation of theoretical minimum drag coefficients, using Eq. 14, and appropriate values of  $C_{Dn}$ . For comparison, the experimental values of minimum drag are also given.

Table IV

$\sigma$	$C_{Dn}$	$C_{Dn} \cos^3$	$C_{D0}$ (Theor.)	$C_{D0}$ (Exp.)
0	.024	.024	.030	.032
30	.041	.027	.033	.032
60	.120	.014	.020	.019
67.5	.015	.001	.007	.010

The agreement here between theoretical and experimental values is qualitatively good, but is open to the most suspicion for high values of  $\sigma$ . It seems likely that for high sweepback angles the "interference" drag at the center section may become relatively more important. This question of minimum drag certainly requires further investigation.

#### Drag Due to Lift.

A finite-span, subsonic airfoil experiences a drag due to the induced velocities across its span, called the "induced drag", which is proportional to the lift squared. A supersonic airfoil of infinite span (2-dimensional) also experiences a drag due to lift, generally called "wave drag", and also proportional to lift squared. As Busemann points out in his Volta Congress paper<sup>1</sup>, it is unfair to make too sharp a distinction between these two types of drag, as both are due to the pressure distribution over the airfoil associated with the lift. Moreover, an infinite supersonic airfoil with finite lift may have zero drag since  $D/L$  is proportional to  $\alpha$ , and the lift on an infinite wing may be finite at zero angle of attack. In the present case of wings with varying sweepback angle, a drag due to lift is also present, as seen in Fig. 16.

In Fig. 4 is plotted the increase in drag coefficient over its minimum value as a function of lift coefficient squared. It is observed that the experimental points are very nearly on straight lines, i.e.,

$$C_D = A + K C_L^2 \quad (17)$$

It will be noted that from the curves that the constant  $A$  in Eq. 17 is not exactly the experimental minimum drag coefficient,  $C_{D0}$ , as the curves do not go through the origin.

If an attempt is made, as before, to relate the force coefficients in the true air stream to those referred to the normal flow, the increase in normal drag coefficient with normal lift coefficient may be written as

$$\Delta C_{Dn} = K_n C_{Ln}^2 \quad (18)$$

Using Eqs. 7 and 14,

$$\Delta C_D = \frac{K_n}{\cos \sigma} C_L^2 \quad (19)$$

or

$$K = K_n / \cos \sigma \quad (20)$$

For a two-dimensional supersonic wing, the coefficient  $K_n$ , according to the linearized theory, is

$$K_n = \sqrt{Ma_n^2 - 1/4} \quad (21)$$

For a subsonic airfoil,  $K_n$  is a function of aspect ratio, AR, according to

$$K_n = \frac{1}{\pi AR} \quad (22)$$

In estimating these factors for the sweepback wings in the present case, no difficulties appear in the applications to  $\sigma = 0^\circ$  and  $30^\circ$ , for which the normal Mach number is supersonic, but for  $\sigma = 60^\circ$  and  $67.5^\circ$ , the conception of aspect ratio becomes rather indefinite. For the present, these factors will be computed for an aspect ratio based on the part of the wing exterior to the body, using the span normal to the true flow direction. In this case, the aspect ratio for all the airfoils is

$$AR = 3.50/1.50 = 2.33$$

Then using Eq. 20 and either Eqs. 21 or 22, theoretical values of K may be computed. These are listed in Table V, together with the experimental values, determined from the slope of the lines in Fig. 4. Also listed are the values of A necessary to fit Eq. 17, and the true values of experimental minimum drag.

Table V

$\sigma$	K (theor.)	K (exp.)	A	C <sub>D0</sub> (exp.)
0	.35	.33	.033	.032
30	.32	.35	.030	.032
60	.27	.37	.016	.019
67.5	.35	.59	.006	.010

The agreement in the first two cases is qualitatively good, but rather poor in the last two. It seems likely that the concept of normal flow is a considerable oversimplification in this case. If, as is sometimes done in subsonic aeronautics, an "airplane efficiency" e is defined, using Eq. 17,

$$K = \frac{1}{\pi AR e \cos \sigma} \quad (23)$$

then e has the values .73 and .60 for  $\sigma = 60^\circ$  and  $67.5^\circ$  respectively.

#### LIFT-DRAG RATIOS

In Fig. 18 are plotted the L/D ratios computed directly from the data in Figs. 16 and 17. It is clear that very little improvement in L/D occurs with  $\sigma = 30^\circ$ , and  $Ma_n > 1$ , but that improvement becomes very marked for  $\sigma = 60^\circ$  and  $67.5^\circ$ . In the last case, the L/D has been increased roughly 80% over the value with no sweepback.

It can be shown using the simple reasoning of the last two sections that little improvement in L/D should be expected for  $Ma_n > 1$ , indicating that sweepback first becomes advantageous when the leading edge of the wing lies behind the Mach wave. Suppose that the variation of drag with lift for a wing conforms to Eq. 17,

$$C_D = A + K C_L^2 \quad (17)$$

It is quickly shown, then, that the maximum L/D is

$$(C_L/C_D)_m = \frac{1}{2\sqrt{KA}} \quad (24)$$

For  $Ma_n > 1$ , the factors K and A are, using Eqs. 14, 20, and 21,

$$A = C_{Dn0} \cos^3 \sigma + 2C_f \quad (25)$$

$$K = \frac{\sqrt{Ma_n^2 - 1}}{4 \cos \sigma} \quad (26)$$

The minimum normal drag coefficient,  $C_{Dn0}$ , is given by Eq. 15. Remembering that  $Ma_n = Ma \cos \sigma$ , we obtain upon substitution of these results in Eq. 24, and after some simplification,

$$(C_L/C_D)_m = 1/\sqrt{\frac{16}{3}t^2 + \frac{2C_f}{\cos \sigma} \sqrt{Ma^2 \cos \sigma - 1}} \quad (27)$$

This result was obtained by Busemann in his Volta Congress paper. It should be pointed out again that this is valid for  $M \cos \sigma > 1$ ; the thickness ratio of the wing,  $t$ , is measured in a direction parallel to the direction of the true air velocity.

If  $t$  is held constant, independent of  $\sigma$ , as was done in the present series of tests, L/D becomes a maximum at  $Ma \cos \sigma = 1$ , in other words, with the airfoil inclined at exactly the Mach angle. However, two things must be observed: first, the linearized theory breaks down slightly before that condition is reached, so the prediction is not accurate for  $Ma_n = 1$ , and secondly, for the values of  $t$  likely to be of importance, the influence of the second term under the radical in Eq. 27 is small. In the present case, for  $t = .08$

$$\frac{16}{3}t^2 = .084 \quad 2C_f \sqrt{Ma_n^2 - 1} = .008$$

Thus the second term will make a difference of roughly 10% in Eq. 27. Actually the effect did not appear to be even this large, due probably to interference effects not accounted for in the above computation. Therefore, little advantage is to be expected from sweepback until the Mach angle is reached.

For sweepback angles such that  $Ma_n < 1$ , the expression for L/D may be written in a similar form;

$$CD = 2C_f + C_{Dn0} \cos^3 \sigma + \frac{1}{\pi AR e} \frac{C_L^2}{\cos \sigma} \quad (28)$$

from which the maximum L/D is

$$(C_L/C_D)_m = 1/2 \sqrt{\frac{1}{\pi AR e} (C_{Dn0} \cos^2 \sigma + \frac{2C_f}{\cos \sigma})} \quad (29)$$

In this expression, the term  $C_{Dn0}$  is understood to be the subsonic normal flow minimum drag exclusive of skin friction, i.e., the "form drag". The subsonic form drag is also a function of Mach number, rising very rapidly near  $Ma_n = .8$ . As a first approximation, it might be assumed that  $C_{Dn0}$  increases according to the factor  $1/\sqrt{1-Ma_n^2}$ , although this will not indicate a sufficiently rapid rise near  $Ma = .8$ .

It is obvious that as  $\sigma$  approaches  $\pi/2$ , L/D approaches zero. Also, as  $\sigma$  approaches the value for which  $Ma_n = 1$ ,  $C_{Dn0}$  approaches infinity, and L/D again approaches zero. Therefore, a maximum L/D will exist for some  $\sigma$  between  $\pi/2 - \theta$ , and 0, where  $\theta$  is the Mach angle. If  $C_{Di}$  is the value of  $C_{Dn0}$  at  $Ma_n = 0$ , then Eq. 29 becomes

$$(CL/CD)_m = \sqrt{\pi AR e / 4 CD_i} / \sqrt{\frac{\cos^2 \sigma}{1 - Ma^2 \cos^2 \sigma} + \frac{2}{\cos \sigma} \cdot \frac{C_f}{CD_i}} \quad (30)$$

A rough value for the minimum drag of an airfoil at  $Ma_n = 0$  is  $CD = .010$ . If  $C_f = .003$ , then  $CD_i = .0040$ . Using  $Ma = 1.72$ , and  $C_f/CD_i = .75$ , the function in Eq. 30 has a maximum near  $\sigma = 60^\circ$ . However, a more accurate estimate of the rapid rise of  $CD_{n0}$  in this vicinity would probably shift the maximum to the right. The function is plotted in Fig. 5 for the values  $AR = 2.33$ ,  $e = .65$ ,  $CD_i = .0040$ . Also plotted are the values of L/D computed from Eq. 27 valid for  $Ma_n > 1$ .

It will be noted that the experimental values of L/D conform very closely to the theoretical for  $Ma_n > 1$ . The point for  $\sigma = 60^\circ$  lies below the curve, which is probably due to the fact that for values of  $Ma_n$  above .8, the rise in normal drag coefficient is much more rapid than that predicted by the factor used above. It must be emphasized that the attempt to express L/D in the form of Eq. 30 with a constant AR and  $e$ , is probably a large over-simplification, and the curve of Fig. 5 should be regarded as only a qualitative indication of the variation of L/D. However, it seems very likely that the value of L/D measured at  $\sigma = 67.5^\circ$  is near the maximum attainable.

It should also be mentioned that another series of four models was similarly tested, identical to the first except that the wings were swept forward instead of back. The principal result was that almost no change in L/D appeared through the entire range of sweep-forward angles. It may be concluded therefore, that there is a fundamental difference in the type of flow in the two cases, and that no advantage is obtained with swept-forward wings.

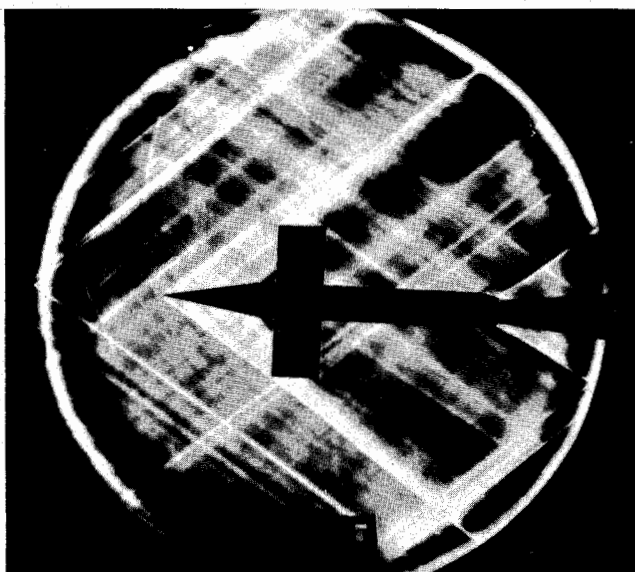


**Fig. 6**  
Model MR58  
 $Ma = 1.72$

**Picture 877**  
 $\alpha = 0^\circ$   
 $\delta = 0^\circ$

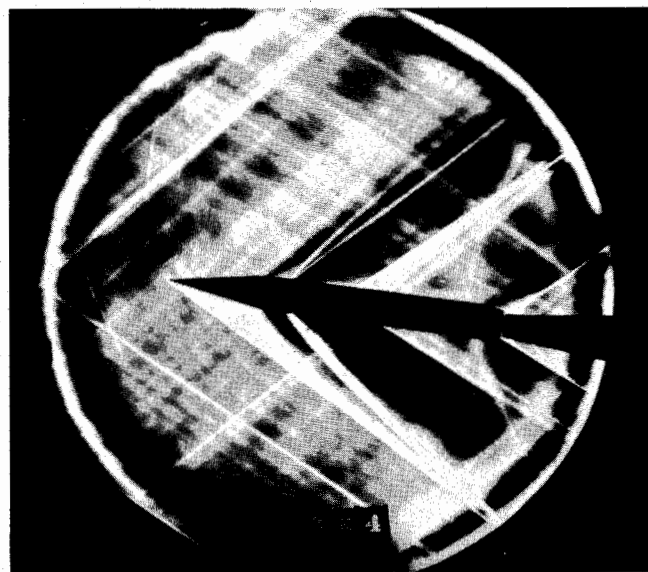


**Fig. 7**  
Model MR58  
 $Ma = 1.72$

**Picture 864**  
 $\alpha = 10^\circ$   
 $\delta = 0^\circ$

### SCHLIEREN OBSERVATIONS OF FLOW

Schlieren photographs were taken of the models, both in side view, and rotated 90° so as to be viewed from the top. In Figs. 6 and 7 are seen the model with  $\alpha = 0^\circ$  from above, and from the side at



Fig. 8  
Model MR60  
 $Ma = 1.72$

Picture 908  
 $\alpha = 0^\circ$   
 $\beta = 60^\circ$



Fig. 9  
Model MR60  
 $Ma = 1.72$

Picture 885  
 $\alpha = 10^\circ$   
 $\beta = 60^\circ$



Fig. 10  
Model MR61  
 $Ma = 1.72$

Picture 1003  
 $\alpha = 0^\circ$   
 $\beta = 67.5^\circ$

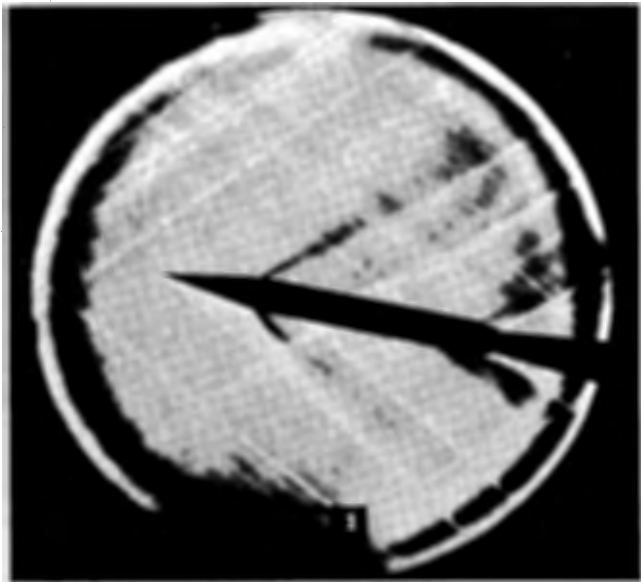
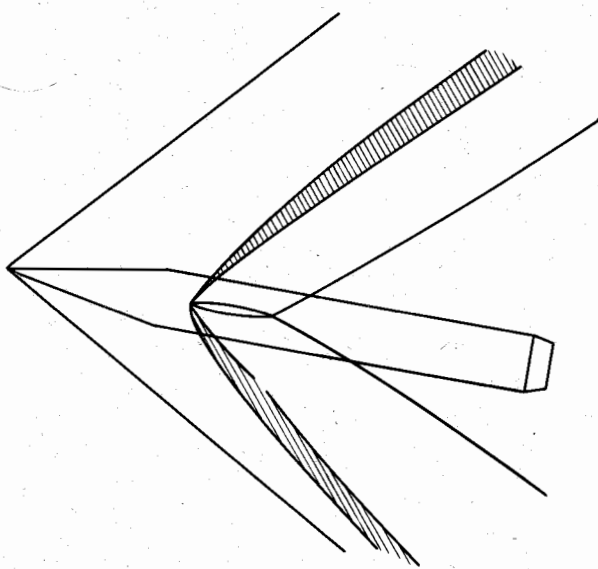


Fig. 11  
Model MR 61  
 $Ma = 1.72$

Picture 991  
 $\alpha = 10^\circ$   
 $\beta = 67.5^\circ$



$$\sigma = 0^\circ, \alpha = 10^\circ$$

FIG. 12

$\alpha = 10^\circ$ . In all pictures, the schlieren knife edge is oriented so that compression from left to right produces a light area in the photograph.

The flow in Fig. 7 is typical of that around a two-dimensional airfoil at an angle of attack, except for several slight modifications due to the fact that the tip of the airfoil is in the conical flow field produced by the nose of the central body. In Fig. 12 the principal elements of this flow are drawn to show their relation to the airfoil. The shock from the leading edge of the lower surface is probably just barely detached, since the angle of attack plus airfoil leading edge angle exceeds the critical angle for  $Ma = 1.72$ .

In Figs. 8 and 9 are top and side views of the model with  $\sigma = 60^\circ$ ,  $\alpha = 10^\circ$ . In Fig. 9, the strong waves of Fig. 7 are strikingly absent, in agreement with expectation. A weak disturbance sheet is seen to emanate from the leading edge of the lower surface and the trailing edge of the upper surface; this is shown more clearly in Fig. 13. It is clear that these waves must have a finite strength at the wing root, which should then diminish toward the tip. The simplified theory discussed previously would not include any drag associated with these waves, which is essentially interference drag.

In Figs. 10 and 11 are shown the model with  $\sigma = 67.5^\circ$  in top and side view at  $\alpha = 10^\circ$ . The flow in the latter is very similar to that of Fig. 9, except that the interference waves are, if anything, weaker. From the schlieren photographs it is clear that the effect of sweepback is to eliminate the large finite shock

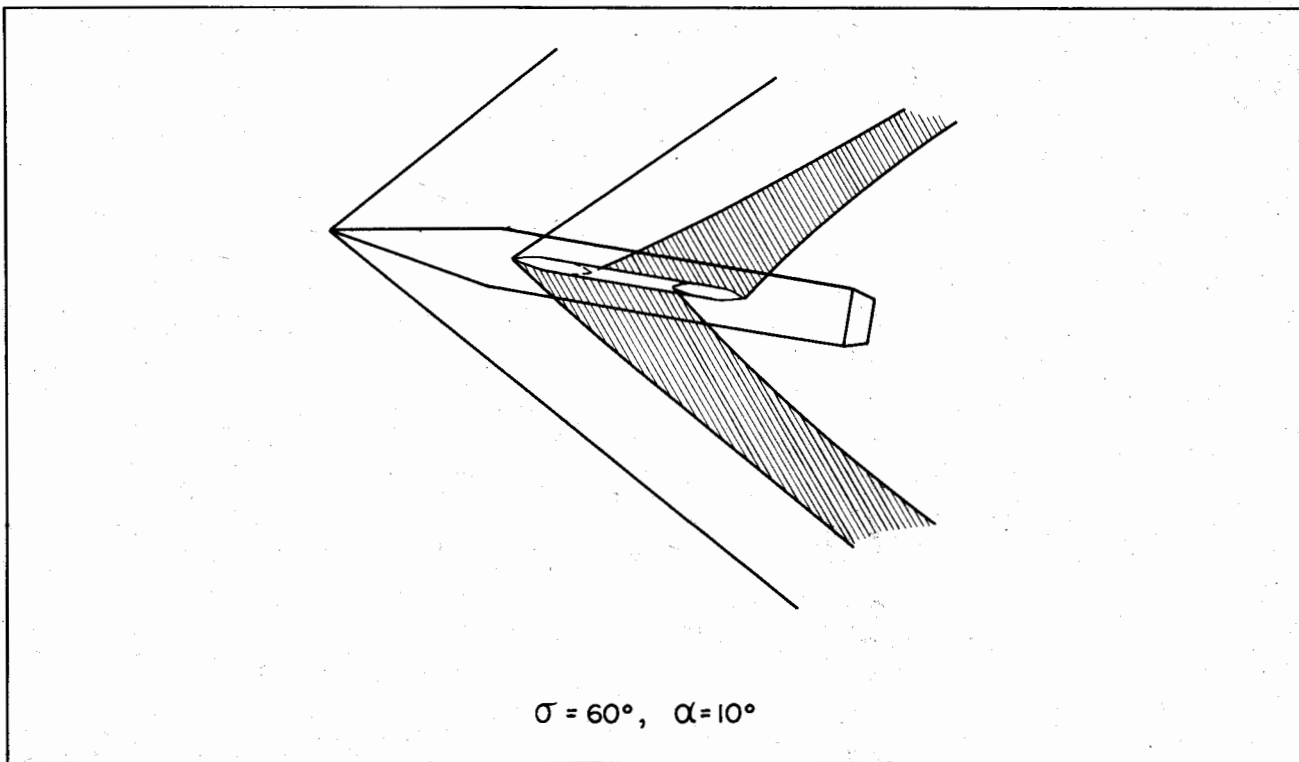


FIG. 13

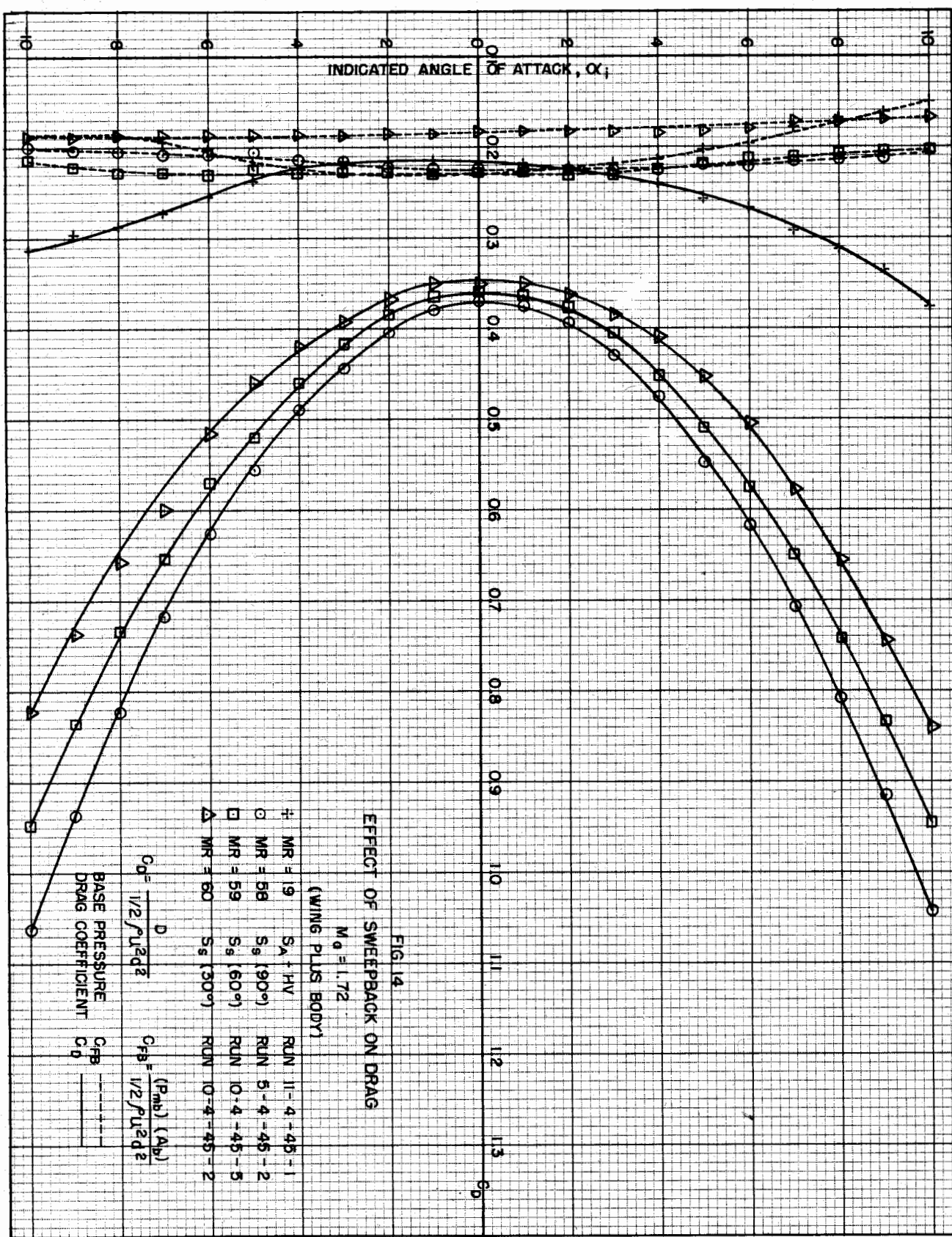
waves associated with the two-dimensional airfoil, which is in accordance with the result of the simplified theory. The presence of the "interference" waves from the wing root reinforces the previous evidence that an accurate computation of the drag of a swept-back wing must include the root effects.

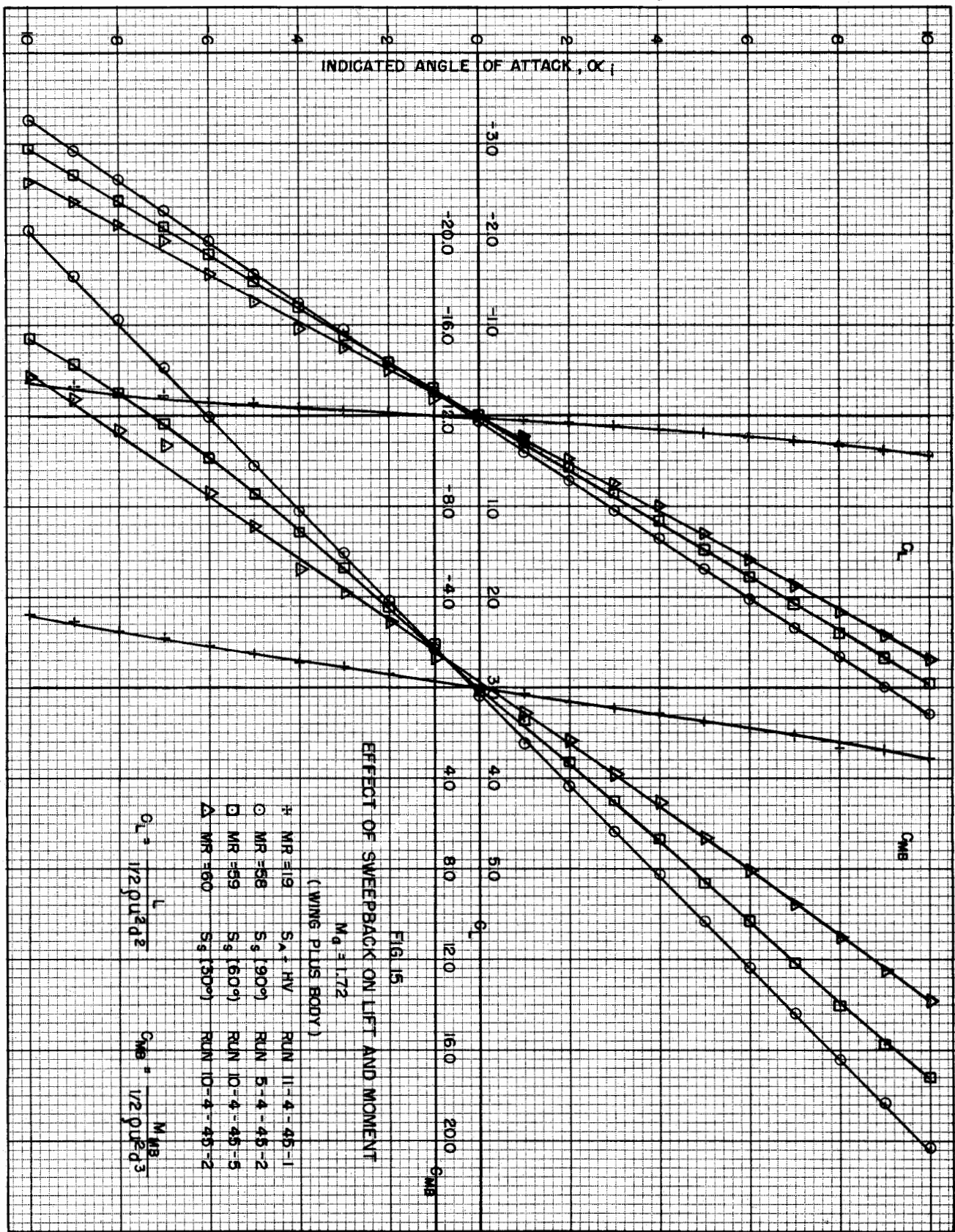
#### CONCLUSIONS

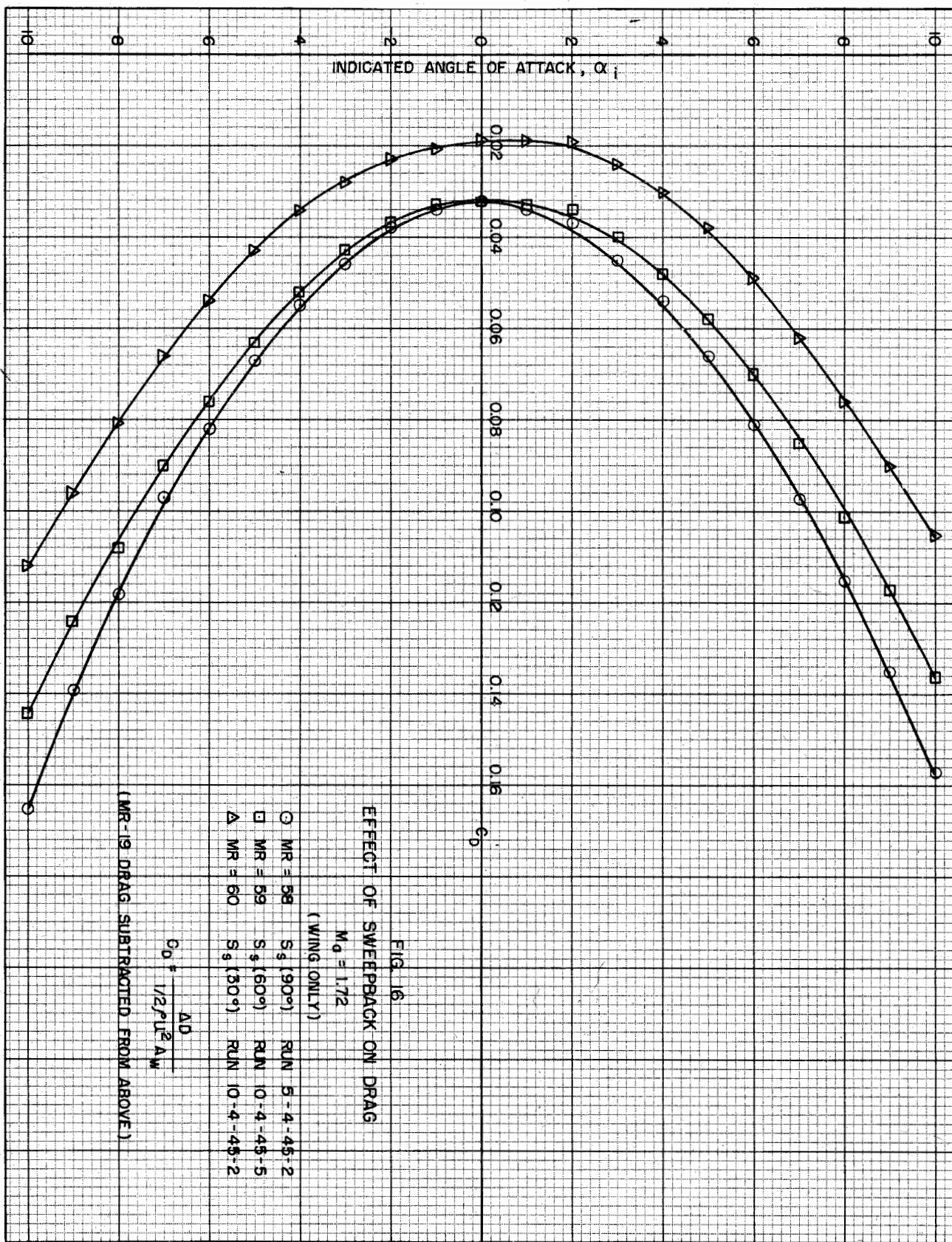
From the above comparisons of test with simple theory, it may be concluded that:

- (1) The aerodynamic characteristics of a swept-back wing may be predicted with reasonable accuracy by computing the two-dimensional characteristics of the wing in the normal component of the true flow, when this normal component is supersonic.
- (2) The qualitative behavior of the aerodynamic characteristics of the wing may be estimated in the same way for a subsonic normal component.
- (3) Very little improvement in L/D is obtained until the normal Mach number becomes less than one, i.e., the wing lies behind the Mach angle.
- (4) The optimum sweepback angle will probably be such that the Mach number of the normal component of the flow lies between .6 and .7.

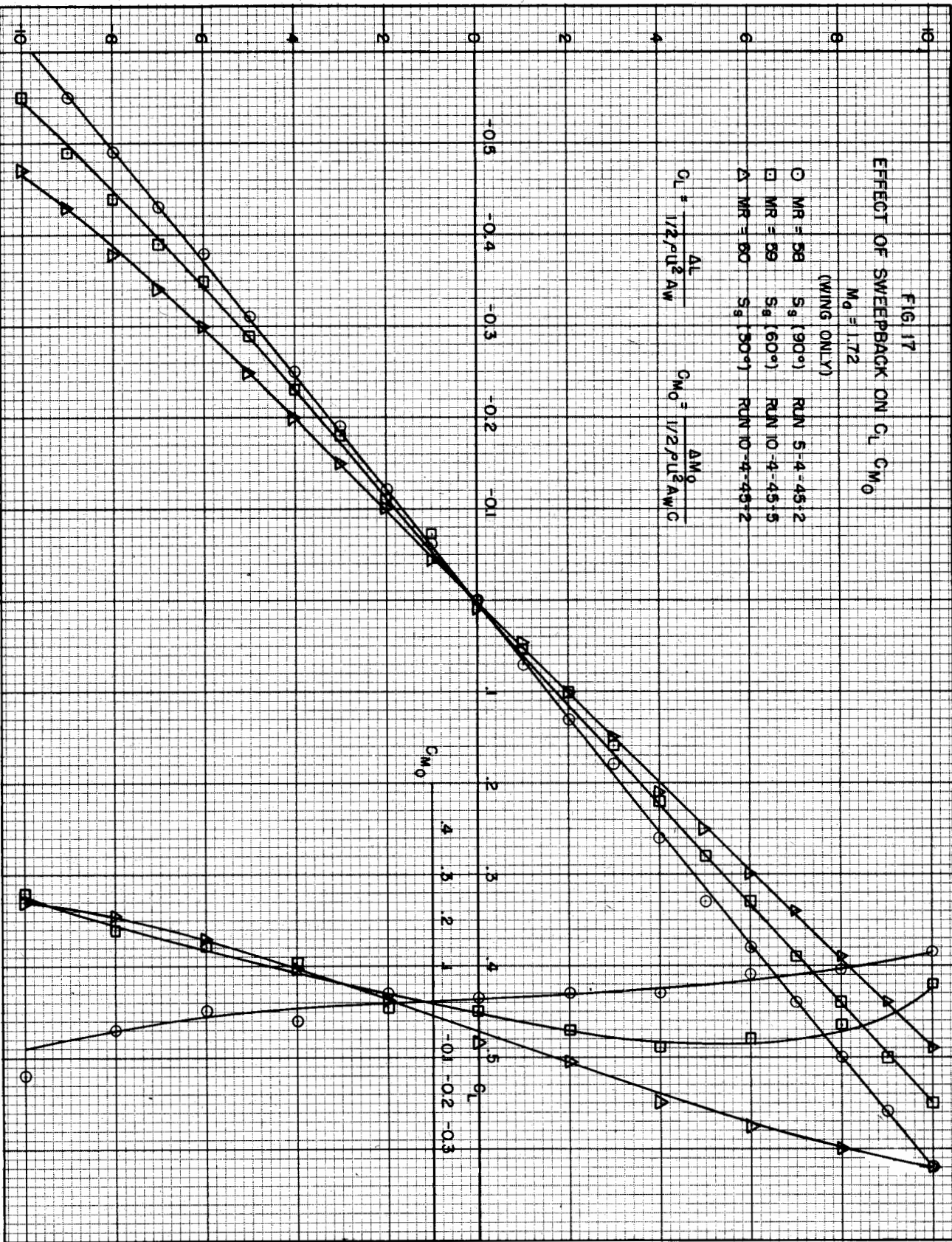
*Allen E. Puckett*







RESTRICTED



RESTRICTED

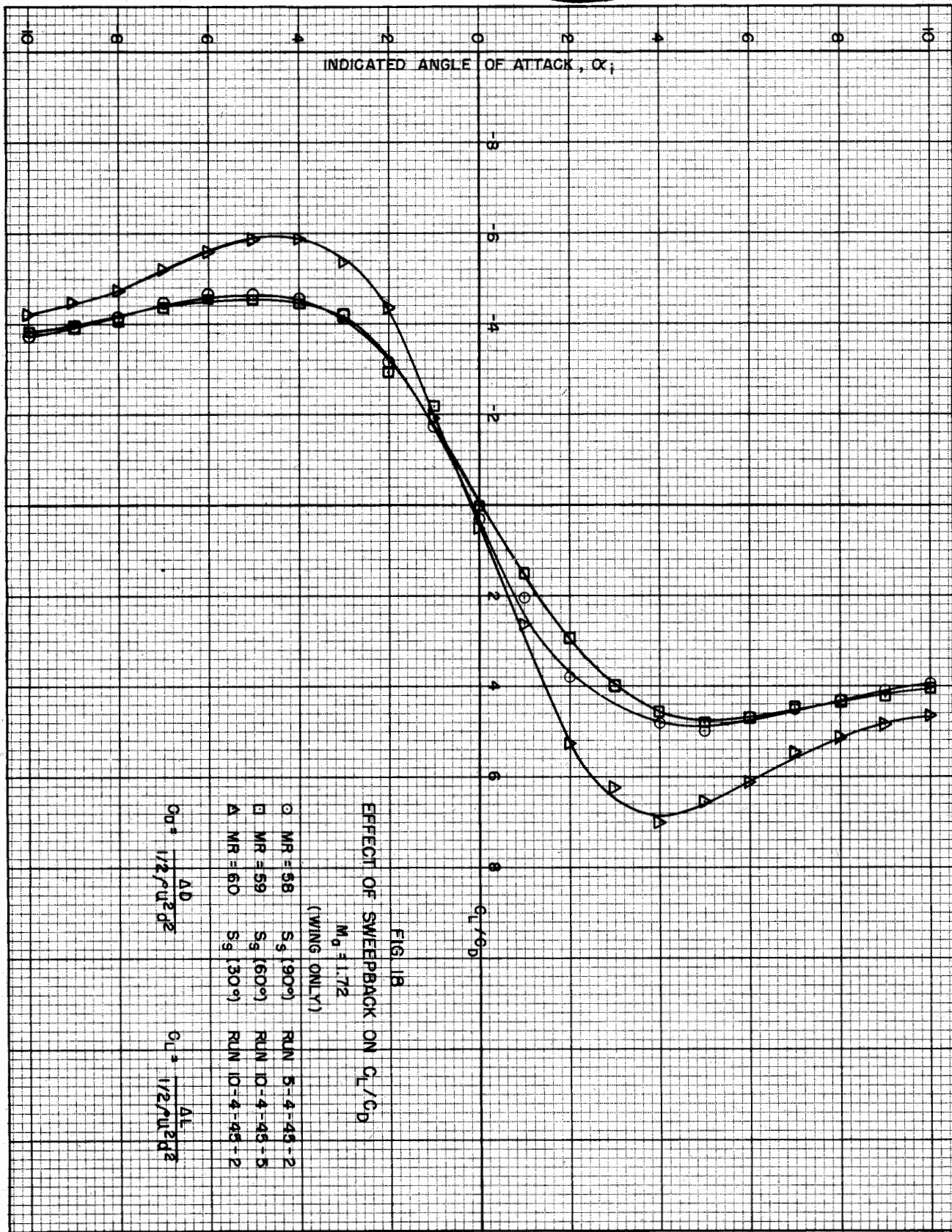


## TABLE OF NOMENCLATURE\*

A	wing area
AR	aspect ratio
C <sub>D</sub>	drag coefficient
C <sub>L</sub>	lift coefficient
C <sub>Mb</sub>	moment coefficient about model base
C <sub>D0</sub>	minimum drag coefficient ( $\alpha = 0$ )
C <sub>FB</sub>	base force coefficient
C <sub>f</sub>	skin friction coefficient
D	drag
K	constant in Eq. 17
K <sub>n</sub>	coefficient
L	lift
Ma	Mach number
M <sub>b</sub>	moment about base of model
Ma <sub>n</sub>	normal Mach number = Ma cos $\sigma$
a <sub>s</sub>	constant defined by Eq. 10a
a <sub>u</sub>	constant defined by Eq. 11
c	wing chord
d	diameter of the model
d'	diameter of the model at the base
e	airplane efficiency
p	local free stream static pressure
p <sub>0</sub>	local free stream stagnation pressure
t	thickness ratio of airfoil relative to longitudinal section of wing
t <sub>n</sub>	thickness ratio of airfoil, normal to chord
u	air velocity
$\alpha$	angle of attack relative to true velocity
$\alpha_n$	normal angle of attack
$\rho$	density of air
$\sigma$	angle of sweepback
$\theta$	Mach angle

\* When the subscript n is used it implies that the force or coefficient is associated with the flow normal to the loading edge of the wing.

~~SECRET~~  
TITLE: Supersonic Wind Tunnel Tests on Four Wings With Sweepback

AUTHOR(S): Puckett, Allen,

ORIGINATING AGENCY: Aberdeen Proving Ground, Aberdeen, Md.

PUBLISHED BY: (Same)

ATI- 6733

DIVISION

(None)

ORIG. AGENCY NO.

BRLR-601

PUBLISHING AGENCY NO.

(Same)

DATE Sept '45	DOC. CLASS. <del>SECRET</del>	COUNTRY U.S.	LANGUAGE English	PAGES 24	ILLUSTRATIONS photos, tables, diagrs, graphs
------------------	----------------------------------	-----------------	---------------------	-------------	---

ABSTRACT:

Four airfoils with different sweepback angles were tested at a Mach number of 1.72 and compared with a simple theory. It was shown that little improvement in lift-drag ratio is produced until airfoil lies inside the Mach angle but that L/D ratio may be almost doubled by using the proper sweepback angle. Discussion is given on lift and drag characteristics and lift-drag ratios. Schlieren observations of flow are presented.

~~Approved and released by [Signature]~~  
~~Attn: [Signature]~~  
~~Central Air Documents Office~~

DISTRIBUTION: Copies of this report obtainable from Central Air Documents Office; Attn: MCJDXD

DIVISION: Aerodynamics (2)

SECTION: Wings and Airfoils (6)

SUBJECT HEADINGS: Wings, Swept-back - Aerodynamics (99305.2); Wings, Swept-back - Drag (99305.7)

ATI SHEET NO.: R-2-6-127

Air Documents Division, Intelligence Department  
Air Materiel Command

AIR TECHNICAL INDEX

~~RESTRICTED~~

Wright-Patterson Air Force Base  
Dayton, Ohio